Structural Studies on Acetylcholinesterase and Paraoxonase Directed Towards Development of Therapeutic Biomolecules for the Treatment of Degenerative Diseases and Protection Agains...

CHAPTER · JANUARY 1970

DOI: 10.1007/978-90-481-2339-1_12

2 AUTHORS, INCLUDING:

Joel Sussman

Weizmann Institute of Science

356 PUBLICATIONS **22,413** CITATIONS

STRUCTURAL STUDIES ON ACETYLCHOLINESTERASE AND PARAOXONASE DIRECTED TOWARDS DEVELOPMENT OF THERAPEUTIC BIOMOLECULES FOR THE TREATMENT OF DEGENERATIVE DISEASES AND PROTECTION AGAINST CHEMICAL THREAT AGENTS

JOEL L. SUSSMAN[1,2*], ISRAEL SILMAN[2,3]
[1]*Department of Structural Biology*
[2]*The Israel Structural Proteomics Center*
[3]*Neurobology Department, Weizmann Institute of Science, Rehovot, Israel*

Abstract. Acetylcholinesterase and paraoxonase are important targets for treatment of degenerative diseases, Alzheimer's disease and atherosclerosis, respectively, both of which impose major burdens on the health care systems in Western society. Acetylcholinesterase is the target of lethal nerve agents, and paraoxonase is under consideration as a bioscavenger for their detoxification. Both are thus the subject of research and development in the context of nerve agent toxicology. The crystal structures of the two enzymes are described, and structure/function relationships are discussed in the context of drug development and of development of means of protection against chemical threats.

Keywords: Alzheimer's disease, catalytic mechanism, crystal-forming variants, directed evolution, organophosphate, nerve agent

1. Introduction

In the following, we will discuss structure/function relationships for two enzymes which share the common feature that they are both associated with major neurodegenerative diseases, and are both relevant to prophylactic and

* To whom correspondence should be addressed. Joel L. Sussman, Department of Structural Biology, Weizmann Institute of Science, Rehovot 76100 ISRAEL; e-mail: joel.sussman@weizmann.ac.il

J.L. Sussman and P. Spadon (eds.), *From Molecules to Medicines*,

therapeutic efforts to overcome what is probably the most potent chemical threat, nerve agent intoxication.

The principal biological role of the synaptic enzyme, acetylcholinesterase (AChE), is to terminate synaptic transmission at cholinergic synapses by rapid hydrolysis of the neurotransmitter, acetylcholine (ACh).[1] In accordance with its biological role, it is an extremely rapid enzyme, operating at a rate at which diffusion control becomes rate-limiting.[2] Organophosphate (OP) nerve agents, and OP and carbamate insecticides, interact rapidly and irreversibly with the human and insect AChEs, respectively, with lethal consequences in both cases.[3,4]

Despite the lethal effects of nerve agents, cholinesterase inhibitors (ChEIs) have been used as drugs since the discovery of the pharmacological properties of the alkaloid, physostigmine, in the 1860s.[5] Interest in the medicinal chemistry of ChEIs intensified when the cholinergic hypothesis was put forward to explain the cognitive impairment characteristic of Alzheimer's disease (AD), the major form of senile dementia.[5,6] According to this hypothesis, cholinergic hypofunction in areas of the brain associated with cognition and memory occurs in AD, and can be symptomatically alleviated by administration of ChEIs. Indeed, all the first generation of drugs for the treatment of AD are ChEIs.[5,7]

Paraoxonase (PON), is a mammalian enzyme that, as its name implies, catalyzes the hydrolysis, and thereby the inactivation, of the insecticide, paraoxon, and of other OPs, such as the nerve agents, soman and sarin.[8,9] One form, PON1, is present in substantial amounts in the serum of humans and other mammals. In recent years it has become apparent that PON1 plays important roles in drug metabolism and in the prevention of the degenerative disease, atherosclerosis.[9,10] Indeed, knockout mice, totally lacking PON1, are highly susceptible both to atherosclerosis and to OP poisoning.[11] *In vitro* assays show that PON1 and the homologous PON3 inhibit lipid oxidation in low-density lipoprotein (LDL, 'bad cholesterol'), thus reducing levels of oxidized lipids that are involved in the initiation of atherosclerosis.[12,13] Because atherosclerosis is the underlying cause of 50% of mortality in Western societies, and OPs present an environmental risk as well as a terrorist threat, PONs have recently become the subject of intensive research.

The name paraoxonase is purely historical, since the PON family is a hydrolase family with one of the broadest specificities known, hydrolyzing OPs, neutral esters and lactones with varying degrees of efficacy. Recent evidence suggests that PON1 is a lactonase,[14] and homocysteine lactone is, indeed, a known risk factor for atherosclerosis.[15]

The solution of the crystal structures of *Torpedo californica* (*Tc*) AChE[16] and, more recently, of a variant of mammalian PON1 obtained by directed evolution,[17] provided the opportunity to obtain a detailed understanding of

structure/function relationships in these two enzymes, which are of crucial importance for design of drugs for the treatment of two of the major degenerative diseases, and for developing approaches for coping with the major chemical threat posed by OP nerve agents.

2. Acetylcholinesterase

The 3D structure of *Tc*AChE displays a number of unexpected features (Fig. 1). Although, as already mentioned, AChE displays very high catalytic activity, especially for a serine hydrolase, its active site is deeply buried, being located almost 20 Å from the surface of the catalytic subunit, at the bottom of a long and narrow cavity. This cavity was named the active-site gorge or, since over 60% of its surface is lined by the rings of conserved aromatic residues, the aromatic gorge.[16,18] Despite the prediction that the catalytic 'anionic' site (CAS), which binds the quaternary moiety of ACh, would contain several negative charges,[19] in fact, only one negative charge is close to the catalytic site, that of E199, adjacent to the active-site serine, S200. Based both upon docking of ACh within the active site[16] and upon affinity labeling,[20] the principal interaction of the quaternary group appears to be a cation-π electron interaction,[21,22] with the indole ring of one of the conserved aromatic residues, W84. A second binding site for ACh at the entrance to the active-site gorge, named the peripheral anionic site (PAS), contains, as its principal residue, another conserved Trp residue, W279. The role of the PAS is to mediate substrate trapping,[23] the trapped ACh then proceeding down the gorge to the CAS. Further inspection reveals that *Tc*AChE possesses an unusually large dipole moment (>1,000 Debye), oriented along the axis of the active-site gorge, whose direction is such as to attract the positively charged substrate, ACh, down the gorge towards the active site.[24] Subsequent solution of the 3D structures of mouse AChE,[25] human AChE[26] and *Drosophila* AChE[27] showed that they all share these general features.

During the 18 years since the 3D structure of *Tc*AChE was solved, we have solved the structures of over 40 complexes and conjugates of a broad repertoire of inhibitors with this enzyme. In most cases, they were obtained by soaking the inhibitor into native crystals, but in a few cases co-crystallization was necessary, usually when crystal-packing constraints did not permit the ligand to occupy its binding site. The complexes formed with reversible inhibitors fall into three categories: (1) Ligands that bind at the active site at the bottom of the gorge; many of these are tertiary or quaternary amines that interact with the CAS; (2) Ligands that bind at the top of the gorge; these are known as 'peripheral site' ligands, since they interact with the PAS; (3) Ligands that span the gorge, containing aromatic and/or tertiary/quaternary

amine moieties, linked by a spacer of a suitable length to permit them to span the CAS and the PAS.[7] The conjugates whose structures were solved were those of several potent OP nerve agents,[28,29] and of the anti-Alzheimer drug, rivastigmine (Exelon™), which is a carbamate.[30] All these compounds inactivate the enzyme irreversibly by attaching covalently to S200. In the following we will present the 3D structures of some prototypic complexes and conjugates, and discuss structure/function relationships.

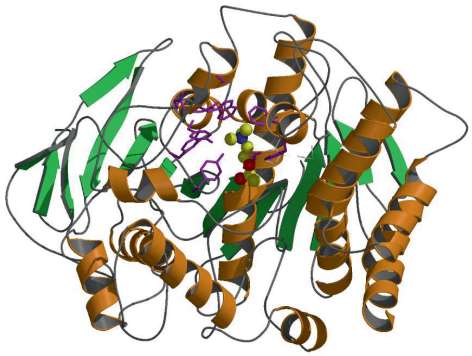

Figure 1. Ribbon diagram showing the 3D structure of *Tc*AChE. Conserved aromatic residues in the active-site gorge are represented as stick models, and ACh is shown as a space-filling model docked at the active site.

2.1. CONJUGATES

Conjugates with OP nerve agents were obtained by soaking the relevant OPs – sarin, soman and VX – into crystals of native *Tc*AChE.[28,29] The structures obtained initially, with sarin and soman, were those of 'aged' conjugates, i.e. of conjugates in which the bound OP moiety had undergone rapid and spontaneous dealkylation.[28,29] The structures of these conjugates revealed the exquisite fit of the OP moiety into the active site, which accounts for the potency of these highly toxic compounds. Thus, in addition to the covalent bond with S200, they make intimate interactions with the acyl pocket and with the oxyanion hole, and the nucleophilic oxygen generated by dealkyation makes a salt bridge with the imidazole of the catalytic histidine, H440.

In the case of VX, 'aging' is a very slow reaction, occurring on a time scale of weeks at 4°C. This permitted collection of structural data for the 'non-aged' conjugate immediately after soaking VX into the *Tc*AChE crystals, and for the non-aged conjugate a few weeks after soaking.[28] It was observed that insertion of the bulky OP moiety into the active site resulted in disruption of the catalytic triad. The H-bond between H440 and E327 was broken, and H440 formed a novel H-bond with E199, adjacent to the active-site serine. Upon 'aging', *viz.* removal of the ethyl group from the

bound OP moiety, the H440-E327 H-bond was concomitantly restored (Fig. 2). Whereas OP conjugates with AChE are, in general, very stable, conjugates produced with carbamates usually turn over on a time scale of minutes.[31] The carbamyl conjugate of rivastigmine (Exelon™) with various AChEs, including the human enzyme, reactivates very slowly, and this may be partially responsible for the effectiveness of this drug.[30,32] Examination of the 3D structure of the conjugate of rivastigmine with *Tc*AChE revealed a structural basis for the slow reactivation observed. Just as in the conjugate with VX referred to above, the H440-E327 H-bond was disrupted; furthermore, the bulky aromatic [(dimethylamino)ethyl]phenol leaving group is retained in the active site.[30]

2.2. COMPLEXES

2.2.1. *Ligands binding at the CAS*

A diverse repertoire of ligands bind near the bottom of the active-site gorge. Most of them interact with W84, the principal residue contributing to the CAS, by either a π-cation interaction or a π-π stacking interaction.[7] Thus, edrophonium, a ChEI inhibitor that acts in the peripheral nervous system, and is used in the diagnosis of myasthenia gravis,[33] has a quaternary group that makes a π-cation interaction with W84. However its inhibitory capacity is significantly increased by formation of H-bonds to both S200 and H440 in the catalytic triad of the enzyme[34] (Fig. 3A). Tacrine (Cognex™), the first ChEI utilized for the treatment of Alzheimer's disease, though since discarded due its hepatoxicity,[35] also interacts with W84; but a second aromatic residue, F330, undergoes a conformational change, resulting in the formation of a sandwich in which the tacrine is stacked between the rings of the two aromatic residues[34] (Fig. 3B).

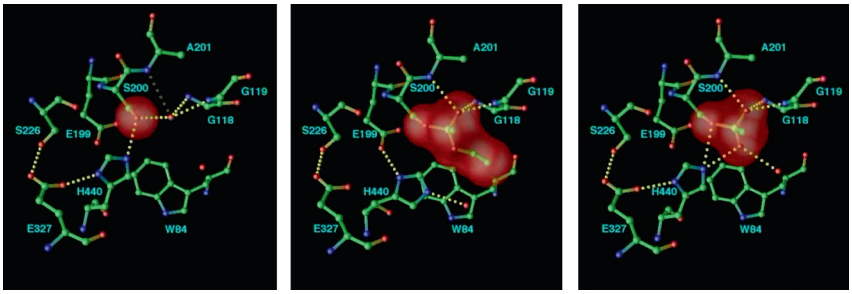

Figure 2. The active-site region in the crystal structures of *Tc*AChE prior to and after inhibition with the nerve agent, VX. (a) Native *Tc*AChE; (b) The 'non-aged' conjugate; (c) The 'aged' conjugate. The polypeptide chain is represented as a stick model, with H-bonds shown as dashed lines. The space-filling models correspond to S200Oγ in (a), to the 'non-aged' OP moiety in (b), and to the 'aged' OP moiety in (c).

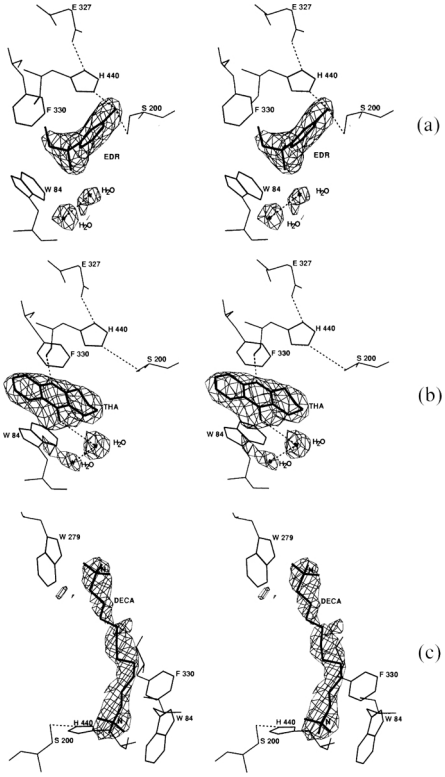

Figure 3. Electron density maps of complexes of *Tc*AChE with (a) edrophonium, (b) tacrine, and (c) decamethonium, showing the principal residues involved in interactions with the ligands. H-bonds are shown as broken lines.

2.2.2. *Ligands binding at the PAS*

Ligands binding specifically at the PAS are, in most cases, quaternary ligands that are too bulky to penetrate the active-site gorge, such as the Indian arrow poison, curare (*d*-tubocurarine),[36] and the fluorescent probe, propidium.[37] At the PAS, also, such ligands interact, via either π-cation or π-π interactions, with the conserved aromatic residues W279 and, to a lesser extent, Y70.[38] But the most striking example of a PAS-specific ligand is the three-fingered polypeptide, fasciculin, found in the venom of the black and green mambas that binds to AChEs from higher vertebrates with affinities in the range of 10^{-10}–10^{-12} M.[39] Solution of the crystal structures of complexes of fasciculin with *Tc*AChE,[40] mouse AChE[25] and human AChE,[26] revealed that the toxin completely covers the entrance to the active-site gorge (Fig. 4), displaying an unusually large contact area with the enzyme (>2,000 Å^2). Despite this large contact area, a crucial interaction between toxin and enzyme is that between the sulphur atom of M33 in the toxin and the indole

group of W279 in *Tc*AChE (or the equivalent Trp residue in the mammalian AChEs). Mutation of this Trp residue results in a decrease of six orders of magnitude in the affinity of the toxin for the enzyme (Radic et al., 1994),[62] which explains its very low affinity for butyrylcholinesterase and for AChE of lower vertebrates, in which this residue is lacking.

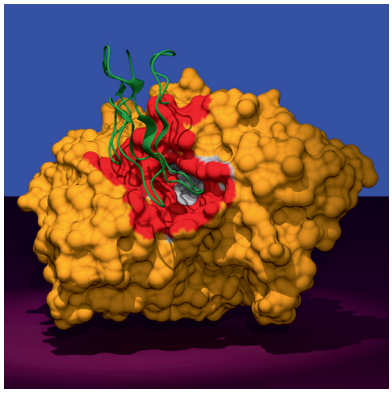

Figure 4. Crystal structure of the complex of fasciculin-II with human recombinant AChE. The molecular surface of the AChE molecule, with residues <4.0 Å from the fasciculin molecule rendered in dark grey, and residues within the active-site gorge rendered in white. The fasciculin molecule is displayed as a ribbon.

2.2.3. *Bifunctional gorge-spanning ligands binding at both the CAS and the PAS*

It has been shown in recent years that AChE can accelerate the assembly of the Aβ peptide to amyloid fibrils.[41,42] The inhibition of this process by propidium suggested that the PAS was responsible for this phenomenon. This raised the possibility that suitable gorge-spanning ligands could display a dual action as anti-Alzheimer drugs, serving as ChEIs at the CAS, and retarding assembly of Aβ to toxic amyloid fibrils at the PAS. This generated considerable interest in the medicinal chemistry of gorge-spanning ligands,[43,44] and in the development of bifunctional ligands that indeed displayed the capacity to inhibit both functions *in vitro*.[45] Furthermore, other categories of gorge-spanning ligands were developed in which the entity binding at the PAS served to inhibit another biological activity associated with neurodegeneration, such as monoamine oxidase,[46] as well as, most recently, gorge-spanning ligands with trifunctional capabilities.[47]

The prototypic gorge-spanning ligand is decamethonium, the ganglionic blocker in which two quaternary ammonium groups are separated by a decamethylene spacer,[48] thus permitting optimal interaction with both W84 and W279 of *Tc*AChE[34] (Fig. 3C). But in terms of utilizing the structural features of the active-site gorge of AChE for optimal drug-target interaction, the anti-Alzheimer drug E2020 (donepezil; Aricept™)[49] serves as an

ideal paradigm. Figure 5 displays the detailed interactions of E2020 with *Tc*AChE as revealed by the crystal structure of the E2020/*Tc*AChE complex.[50] At the bottom of the gorge, the benzyl group of the drug stacks against W84, midway up the gorge the tertiary nitrogen of the piperidine ring makes a cation-π interaction with the phenyl ring of F330, and at the top of the gorge, the 5,6-dimethoxy-2,3-dihydroinden-1-one moiety stacks against W279. Interestingly, there are no direct H-bonds or salt bridges between the drug and the enzyme; but H-bonds are formed between the ligand and conserved water molecules within the active-site gorge[51]; these, in turn, form H-bonds with amino acid residues of the protein. Thus, in terms of drug design, the conserved water molecules can be considered as an integral part of the template formed by the surface of the gorge.

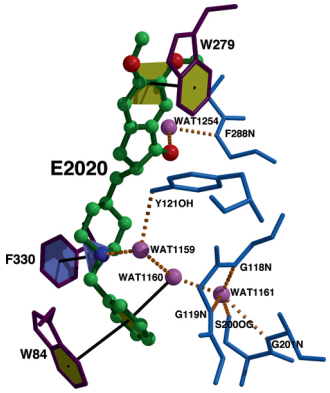

Figure 5. Binding modes of E2020 to *Tc*AChE. E2020 is displayed as a ball-and-stick model; water-mediated binding residues as light grey sticks, water molecules as light grey balls, "standard" H-bonds as heavy dashed lines, aromatic H-bonds, π cation and π–π stacking interactions as dark lines.

3. Paraoxonases

3.1. CRYSTALLIZATION AND STRUCTURE DETERMINATION

Human PON1 is rather unstable, and tends to aggregate in the absence of detergents.[52] Nor is it amenable to functional expression in bacteria or yeast, and thus to mutagenesis, library selection, and protein engineering. These factors led us to directly evolve PONs for bacterial expression and increased solubility.[53] Family shuffling of four PON1 genes (human, rabbit, mouse and rat) (Fig. 6), followed by screening for esterolytic activity, led to recombinant PON1 variants (rePON1s) that are expressed well in *E. coli*. These variants diverged from the wild-type (wt) rabbit PON1 by 14-32 amino acids contributed by the other three PON1 genes. The rePON1 variants exhibited enzymatic properties essentially identical to those of the

wt PON1,[53] and similar biological activities in inhibiting LDL oxidation and mediating cholesterol efflux from macrophages.[54,55] Variants from the first round of evolution displayed a tendency to aggregate, and none could be crystallized. The second-generation variants, obtained by shuffling of the first-generation variants and screening for highest expression levels, did not aggregate, and one (G2E6) yielded stable well-diffracting crystals.

RePON1-G2E6 exhibits 91% homology to wt rabbit PON1 (Fig. 6), with the majority of the variations deriving from human, mouse, or rat weight PON1. Rabbit and human PON1s are also highly homologous in

```
PON1_RABBIT        MAKLTALTLLGLGLALFDGQKSSFQTRFNVHREVTPVELPNCNLVKGIDNGSEDLEILPN
G2E6               -----------M------R-----------------------------------------
G1C4               ----L----V-----------------------------------------ET-A--------
G3C9               ---------------------------------------------V-------------
G3H8               ------P-----------R-----------------------------------------
P1D6               ------------------R-----------------------------------------
P2D4               ------------------R-----------------------------------------

PON1_RABBIT        GLAFISSGLKYPGIMSFDPDKSGKILLMDLNEEDPVVLELGITGSTFDLSSFNPHGISTF
G2E6               -------------------------------KE-A-S--E-I-N-L-I------------
G1C4               ------------------------------------------------------------
G3C9               ----------------------------------------------N-L-I------------
G3H8               ------------------------------------------------------------
P1D6               ------------------------------------------------------------
P2D4               ------------------------------------------------------------

PON1_RABBIT        TDEDNIVYLMVVNHPDSKSTVELFKFQEKEKSLLHLKTIRHKLLPSVNDIVAVGPEHFYA
G2E6               I-D--T---L-----G-S----V-----E-------------------------------
G1C4               -----T---L-------S----V-----E-------------------------------
G3C9               -----T---L-------S----V-----E-------------------------------
G3H8               -----T---L-------S----V-------------------------------------S---
P1D6               -----T---L-------S----V-------R-------------------------S---
P2D4               ---------M------------------E-R-------------------------S---

PON1_RABBIT        TNDHYFIDPYLKSWEMHLGLAWSFVTYYSPNDVRVVAEGFDFANGINISPDGKYVYIAEL
G2E6               ------------------------------------------------------------
G1C4               ------------------------------------------------------------
G3C9               ------------------------------------------------------------
G3H8               ------A-----------------------------------------------------
P1D6               ------A-----------------------------------------------------
P2D4               ------------------------------------------------------------

PON1_RABBIT        LAHKIHVYEKHANWTLTPLKSLDFNTLVDNISVDPVTGDLWVGCHPNGMRIFYYDPKNPP

G2E6               -------------------RV-S-D---------------------------F--AE---
G1C4               ------------------------------------------------------------
G3C9               ------------------------D-------------------------------------
G3H8               ------------------------------------------------------------
P1D6               ------------------------------------------------------------E---
P2D4               --------------------V-N-D---------------------------F--AE---

PON1_RABBIT        ASEVLRIQDILSKEPKVTVAYAENGTVLQGSTVAAVYKGKMLVGTVFHKALYCEL
G2E6               G-----------E------V--------------------L-I----------D-
G1C4               ------------ED--I--V----------T---S-----L-I----------D-
G3C9               G-----------E------V--------------------L-I------------
G3H8               G------------------V--------------------L-I----------D-
P1D6               G------------------V--------------------L-I----------D-
P2D4               G------------------V--------------S-----L-I----------D-
```

Figure 6. Sequence alignment of rabbit PON1 with six variants showing only residues differing from those in wild type rabbit PON1. G2E6 is the variant whose structure was solved, with its unique residues highlighted.

sequence (86 %) and function.[56] Sequence variations between rePON1-G2E6 and rabbit and human PON1 are in regions that do not affect their active sites.

The refined 2.2 Å crystal structure of rePON1 (R 18.5%; R_f 21.7%) contains one molecule per asymmetric unit. It was solved by single isomorphous replacement anomalous scattering (SIRAS) using a selenomethionine (SeMet) construct. The structure shows all residues except residues 1–15 at the N-terminus, and a surface loop (residues 72–79). Two calcium atoms, a phosphate ion, and 115 water molecules are also seen.

3.2. RABBIT PON1 VS. THE G2E6 VARIANT OBTAINED BY DIRECTED EVOLUTION

Figure 7 displays the crystal structure of the G2E6 variant, which shows 31 of the 32 residues that are mutated relative to the rabbit PON1 sequence (the mutation in residue 12 is in the N-terminal sequence that fails to display electron density). Twenty-two of these differences are on the surface of the molecule, and nine are in the core. The inner core mutations are from one hydrophobic residue to another. It has been suggested that the enhanced stability of G2E6 is due to three mutated residues, which are common to all the variants for which crystallization experiments were performed (Fig. 7). These are M341L and V343I, both hydrophobic core residues that pack

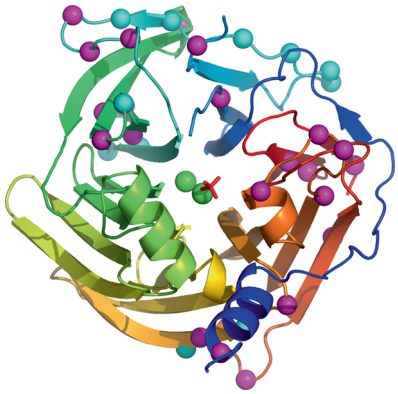

Figure 7. Ribbon diagram of the 6-bladed β-propeller structure of the rePON1 variant G6E2. The variant's mutated residues, relative to WT rabbit PON1, are shown as dark and light balls, light balls indicating unique mutations in G2E6 not shared by the five other variants of PON1 that failed to crystallize. The two Ca ions are shown as balls at the center of the structure, and the phosphate ion as a stick model. The two blades in the left-hand portion of the structure are mutation-free.

against each other, and the neighbouring A320V. It has been proposed[57] that these mutations increase the stability of the calcium-free apo-form of PON1.

Detergent-solubilized PON1 forms dimers and higher oligomers,[52] but there is only one molecule per asymmetric unit of the crystal, and very few contacts between symmetry-related molecules. It is possible that crystallization favours a monomeric form.

3.3. THE CATALYTIC MECHANISM

The upper of the two calcium ions seen in the crystal structure, Ca-1, lies at the bottom of the active-site cavity, together with a phosphate ion coming from the mother liquor.[17] One of this phosphate's oxygens is only 2.2 Å from Ca-1. This phosphate ion may be bound in a mode similar to the intermediates in the hydrolytic reactions catalyzed by PON, with the oxygen adjacent to Ca-1 mimicking the oxyanionic moiety of those intermediates stabilized by the positively-charged calcium ion. This type of "oxyanion hole" is seen in secreted phospholipase A2,[58] and has also been suggested for diisopropylfluorophosphatase,[59] whose overall structure closely resembles that of PON1. Two other phosphate oxygens may be mimicking the attacking hydroxyl ion and the oxygen of the alkoxy or phenoxy leaving groups of ester and lactone substrates.

To help elucidate PON1's mechanism, we determined its catalytic pH-rate profile. The pH-dependence observed may be ascribed to a histidine imidazole involved in a base-catalyzed, rate-determining step. In hydrolytic enzymes, histidine often serves as a base, deprotonating a water molecule, and thus generating the attacking hydroxide ion that produces hydrolysis.

A His-His dyad was identified near both Ca-1 and the phosphate ion (Fig. 8). We hypothesize that H115, the closer nitrogen of which is only 4.1 Å from Ca-1, acts as a general base to deprotonate a single water molecule, thus generating the attacking hydroxide, while H134 acts in a proton shuttle mechanism to increase H115's basicity. Interestingly, H115 adopts distorted dihedral angles - a phenomenon observed in catalytic residues of many enzymes. In support of the postulated mechanism we investigated the H115Q, H115A, and H115W mutations, all of which produce a dramatic decrease in both arylesterase and lactonase activity of PON1, and the H134Q mutation, which resulted in a milder, yet significant, decrease. Interestingly, the paraoxonase activity of the PON1 variant was not affected by any of these His mutations.[55]

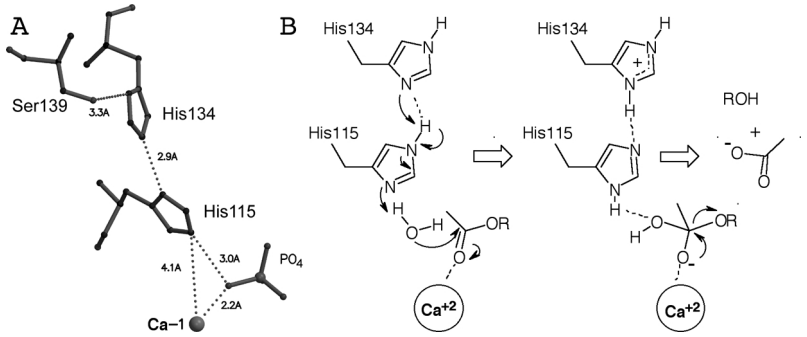

Figure 8. The postulated catalytic site and mechanism of PON1. (A) The catalytic site: the upper calcium atom (Ca-1), the phosphate ion at the bottom of the active site, and the postulated His-dyad; (B) Schematic representation of the proposed mechanism of action of PON1 on ester substrates such as phenyl and 2-naphthylacetate. The first step involves deprotonation of a water molecule by the His dyad to generate a hydroxide anion which attacks the ester carbonyl, producing an oxyanionic, tetrahedral intermediate. This intermediate breaks down (second step) to an acetate ion and either phenol or 2-naphthol.

3.4. DISCUSSION AND CONCLUSIONS

This study complements earlier examples of the application of directed evolution for protein crystallization.[60] Directed evolution was also applied to identify PON1's active site, and provided key insights as to how the substrate selectivity of the PON family members evolved in nature. Two thirds of the mutations in the G62E mutant are found on the surface of the molecule. The alignment of all the PON1 variants that were subjected to crystallization trials (Fig. 6) shows that the crystallized variant G2E6, which was crystallized successfully, has about twice as many mutations as those, which could not be crystallized. Thus, it bears 32 mutations vs. 13–19 mutations for the three variants that did not crystallize. Ten of these mutations are unique to the G2E6 variant. They are all located on the surface of PON1, yet they do not make contacts with symmetry-related molecules in the crystal. The present study shows the advantage of directed evolution in generating a range of variants that are very similar, of which only some may readily form crystals. The mutations in the G2E6 variant are spread throughout most of the molecule, except for two blades of the six-bladed β-propeller, blades 3 and 4, neither of which bears a mutation (Fig. 7). Detergent-solubilized PON1 forms dimers and higher oligomers,[52] although the crystal structure contains only one monomer in the asymmetric unit. It is possible that the mutation-free surface is the site of dimerization of the PON1, being in this respect similar to the highly soluble bacterial phosphotriesterase variants which contain only three point mutations, all of which are distal from the dimer surface[61]; i.e., in this latter case the dimer surface is also mutation-free.

The crystal structure unravels both the overall fold of the PON family and the details of PON1's structure. It permits postulation of the catalytic mechanism of the esterase and lactonase functions of PONs. The mutagenesis data[55] indicate that these two activities of PON1 are catalyzed by a H115-H134 dyad, while the paraoxonase activity is not affected by the dyad mutations and, hence, must be catalyzed by residues which have yet to be identified.

The directed evolution results demonstrate the remarkable evolvability of this enzyme family, and its impact on obtaining active, stable, and soluble protein variants that are amenable to crystallization and to subsequent 3-D structure determination.

ACKNOWLEDGEMENTS

We acknowledge financial support by Autism Speaks, the Nalvyco Foundation, the Bruce Rosen Foundation, a research grant from Mr. Erwin Pearl, the Jean and Jula Goldwurm Memorial Foundation, the Kimmelman Center for Biomolecular Structure and Assembly, and the Minerva Foundation to JLS, by the Benziyo Center for Neuroscience to IS, by the Israel Science Foundation to IS & JLS, and by Grant Number U54NS058183 from the National Institute of Neurological Disorders and Stroke and the Defense Threat Reduction Agency (DTRA) of the US Army. The structures were determined in collaboration with the Israel Structural Proteomics Center (ISPC), supported by the Israel Ministry of Science, Culture and Sport, the Divadol Foundation, the Neuman Foundation, the European Commission Sixth Framework Research and Technological Development Programme 'SPINE2-COMPLEXES' Project under contract No. 031220, and the 'Teach-SG' Project, under contract number ISSG-CT-2007-037198. JLS is the incumbent of the Morton and Gladys Pickman Chair of Structural Biology.

References

1. Rosenberry, T. L., Acetylcholinesterase, *Adv. Enzymol.* 43, 103–218 (1975).
2. Quinn, D. M., Acetylcholinesterase: enzyme structure, reaction dynamics, and virtual transition states, *Chem. Rev.* 87, 955–975 (1987).
3. Millard, C. B. & Broomfield, C. A., Anticholinesterases: medical applications of neurochemical principles, *J. Neurochem.* 64, 1909–1918 (1995).
4. Casida, J. E. & Quistad, G. B., Golden age of insecticide research: past, present, or future?, *Annu. Rev. Entomol.* 43, 1–16 (1998).
5. Giacobini, E. Cholinesterases Inhibitors: from the Calabar bean to Alzheimer therapy. In *Cholinesterases and Cholinesterase Inhibitors* (Giacobini, E., ed.), pp. 181–226. Martin Dunitz, London (2000).

6. Bartus, R. T., Dean, R. L. Jr., Beer, B. & Lippa, A. S., The cholinergic hypothesis of geriatric memory dysfunction, *Science* 217, 408–414 (1982).
7. Greenblatt, H. M., Dvir, H., Silman, I. & Sussman, J. L., Acetylcholinesterase: a multi-faceted target for structure-based drug design of anticholinesterase agents for the treatment of Alzheimer's disease, *J. Mol. Neurosci.* 20, 369–384 (2003).
8. Aldridge, W. N., Serum esterases II. An enzyme hydrolysing diethyl *p*-nitrophenyl acetate (E600) and its identity with the A-esterase of mammalian sera, *Biochem. J.* 53, 117–124 (1953).
9. Draganov, D. I. & La Du, B. N., Pharmacogenetics of paraoxonases: a brief review, *Naunyn Schmiedebergs Arch. Pharmacol.* 369, 78–88 (2004).
10. Lusis, A. J., Atherosclerosis, *Nature* 407, 233–241 (2000).
11. Shih, D. M., Gu, L., Xia, Y. R., Navab, M., Li, W. F., Hama, S., Castellani, L. W., Furlong, C. E., Costa, L. G., Fogelman, A. M. & Lusis, A. J., Mice lacking serum paraoxonase are susceptible to organophosphate toxicity and atherosclerosis, *Nature* 394, 284–287 (1998).
12. Mackness, M. I., Arrol, S. & Durrington, P. N., Paraoxonase prevents accumulation of lipoperoxides in low-density lipoprotein, *FEBS Lett.* 286, 152–154 (1991).
13. Reddy, S. T., Wadleigh, D. J., Grijalva, V., Ng, C., Hama, S., Gangopadhyay, A., Shih, D. M., Lusis, A. J., Navab, M. & Fogelman, A. M., Human paraoxonase-3 is an HDL-associated enzyme with biological activity similar to paraoxonase-1 protein but is not regulated by oxidized lipids, *Arterioscler. Thromb. Vasc. Biol.* 21, 542–547 (2001).
14. Khersonsky, O. & Tawfik, D. S., Structure-reactivity studies of serum paraoxonase PON1 suggest that its native activity is lactonase, *Biochemistry* 44, 6371–6382 (2005).
15. Jakubowski, H., Calcium-dependent human serum homocysteine thiolactone hydrolase. A protective mechanism against protein N-homocysteinylation, *J. Biol. Chem.* 275, 3957–3962 (2000).
16. Sussman, J. L., Harel, M., Frolow, F., Oefner, C., Goldman, A., Toker, L. & Silman, I., Atomic structure of acetylcholinesterase from *Torpedo californica*: a prototypic acetylcholine-binding protein, *Science* 253, 872–879 (1991).
17. Harel, M., Aharoni, A., Gaidukov, L., Brumshtein, B., Khersonsky, O., Meged, R., Dvir, H., Ravelli, R. B., McCarthy, A., Toker, L., Silman, I., Sussman, J. L. & Tawfik, D. S., Structure and evolution of the serum paraoxonase family of detoxifying and anti-atherosclerotic enzymes, *Nat. Struct. Mol. Biol.* 11, 412–419 (2004).
18. Axelsen, P. H., Harel, M., Silman, I. & Sussman, J. L., Structure and dynamics of the active site gorge of acetylcholinesterase: synergistic use of molecular dynamics simulation and X-ray crystallography, *Protein Sci.* 3, 188–197 (1994).
19. Nolte, H. -J., Rosenberry, T. L. & Neumann, E., Effective charge on acetylcholinesterase active sites determined from the ionic strength dependence of association rate constants with cationic ligands, *Biochemistry* 19, 3705–3711 (1980).
20. Weise, C., Kreienkamp, H. -J., Raba, R., Pedak, A., Aaviksaar, A. & Hucho, F., Anionic subsites of the acetylcholinesterase from *Torpedo californica*: affinity labelling with the cationic reagent *N,N*-dimethyl-2-phenyl-aziridinium, *EMBO J.* 9, 3885–3888 (1990).
21. Dougherty, D. A. & Stauffer, D. A., Acetylcholine binding by a synthetic receptor: implications for biological recognition, *Science* 250, 1558–1560 (1990).
22. Dougherty, D. A., Cation-π interactions in chemistry and biology: a new view of benzene, phe, tyr, and trp, *Science* 271, 163–168 (1996).
23. Rosenberry, T. L., Johnson, J. L., Cusack, B., Thomas, J. L., Emani, S. & Venkatasubban, K. S., Interactions between the peripheral site and the acylation site in acetylcholinesterase, *Chem. Biol. Interactions* 157–158, 181–189 (2005).

24. Ripoll, D. R., Faerman, C. H., Axelsen, P. H., Silman, I. & Sussman, J. L., An electrostatic mechanism for substrate guidance down the aromatic gorge of acetylcholinesterase, *Proc. Natl. Acad. Sci. USA* 90, 5128–5132 (1993).
25. Bourne, Y., Taylor, P. & Marchot, P., Acetylcholinesterase inhibition by fasciculin: crystal structure of the complex, *Cell* 83, 503–512 (1995).
26. Kryger, G., Harel, M., Giles, K., Toker, L., Velan, B., Lazar, A., Kronman, C., Barak, D., Ariel, N., Shafferman, A., Silman, I. & Sussman, J. L., Structures of recombinant native and E202Q mutant human acetylcholinesterase complexed with the snake-venom toxin fasciculin-II, *Acta Cryst.* D56, 1385–1394 (2000).
27. Harel, M., Kryger, G., Rosenberry, T. L., Mallender, W. D., Lewis, T., Fletcher, R. J., Guss, J. M., Silman, I. & Sussman, J. L., Three-dimensional structures of *Drosophila melanogaster* acetylcholinesterase and of its complexes with two potent inhibitors, *Protein Sci.* 9, 1063–1072 (2000).
28. Millard, C. B., Koellner, G., Ordentlich, A., Shafferman, A., Silman, I. & Sussman, J. L., Reaction products of acetylcholinesterase and VX reveal a mobile histidine in the catalytic triad, *J. Am. Chem. Soc.* 121, 9883–9884 (1999).
29. Millard, C. B., Kryger, G., Ordentlich, A., Harel, M., Raves, M., Greenblatt, H. M., Segall, Y., Barak, D., Shafferman, A., Silman, I. & Sussman, J. L., Crystal structure of "aged" phosphylated *Torpedo* acetylcholinesterase: nerve agent reaction products at the atomic level, *Biochemistry* 38, 7032–7039 (1999).
30. Bar-On, P., Millard, C. B., Harel, M., Dvir, H., Enz, A., Sussman, J. L. & Silman, I., Kinetic and structural studies on the interaction of cholinesterases with the anti-Alzheimer drug rivastigmine, *Biochemistry* 41, 3555–3564 (2002).
31. Aldridge, W. N. & Reiner, E., *Enzyme Inhibitors as Substrates* (Elsevier, New York, 1975).
32. Weinstock, M., Razin, M., Chorev, M. & Enz, A., Pharmacological evaluation of phenylcarbamates as CNS-selective acetylcholinesterase inhibitors, *J. Neural Transm. Suppl.* 43, 219–225 (1994).
33. Karatas, H., Nurlu, G. & Kansu, T., Is there still a role for edrophonium in diagnosing ocular myasthenia, *Eur. J. Neurosci.* 14, e4–5 (2007).
34. Harel, M., Schalk, I., Ehret-Sabatier, L., Bouet, F., Goeldner, M., Hirth, C., Axelsen, P., Silman, I. & Sussman, J. L., Quaternary ligand binding to aromatic residues in the active-site gorge of acetylcholinesterase, *Proc. Natl. Acad. Sci. USA* 90, 9031–9035 (1993).
35. Summers, W. K., Tachiki, K. H. & Kling, A., Tacrine in the treatment of Alzheimer's disease. A clinical update and recent pharmacologic studies, *Eur. Neurol.* 29(Suppl 3), 28–32 (1989).
36. Changeux, J. -P., Responses of acetylcholinesterase from *Torpedo marmorata* to salts and curarizing drugs, *Mol. Pharmacol.* 2, 369–392 (1966).
37. Taylor, P. & Lappi, S., Interaction of fluorescence probes with acetylcholinesterase. The site and specificity of propidium binding, *Biochemistry* 14, 1989–1997 (1975).
38. Bourne, Y., Taylor, P., Radic, Z. & Marchot, P., Structural insights into ligand interactions at the acetylcholinesterase peripheral anionic site, *EMBO J.* 22, 1–12 (2003).
39. Karlsson, E., Mbugua, P. M. & Rodriguez-Ithurralde, D., Fasciculins, anticholinesterase toxins from the venom of the green mamba *Dendroaspis angusticeps*, *J. Physiol. (Paris)* 79, 232–240 (1984).
40. Harel, M., Kleywegt, G. J., Ravelli, R. B. G., Silman, I. & Sussman, J. L., Crystal structure of an acetylcholinesterase-fasciculin complex: interaction of a three-fingered toxin from snake venom with its target, *Structure* 3, 1355–1366 (1995).

41. Inestrosa, N. C., Alvarez, A., Perez, C. A., Moreno, R. D., Vicente, M., Linker, C., Casanueva, O. I., Soto, C. & Garrido, J., Acetylcholinesterase accelerates assembly of amyloid-beta-peptides into Alzheimer's fibrils: possible role of the peripheral site of the enzyme, *Neuron* 16, 881–891 (1996).
42. Bartolini, M., Bertucci, C., Cavrini, V. & Andrisano, V., beta-Amyloid aggregation induced by human acetylcholinesterase: inhibition studies, *Biochem. Pharmacol.* 65, 407–416 (2003).
43. Du, D. M. & Carlier, P. R., Development of bivalent acetylcholinesterase inhibitors as potential therapeutic drugs for Alzheimer's disease, *Curr. Pharm. Des.* 10, 3141–3156 (2004).
44. Haviv, H., Wong, D. M., Silman, I. & Sussman, J. L., Bivalent ligands derived from Huperzine A as acetylcholinesterase inhibitors, *Curr. Top. Med. Chem.* 7, 375–387 (2007).
45. Belluti, F., Rampa, A., Piazzi, L., Bisi, A., Gobbi, S., Bartolini, M., Andrisano, V., Cavalli, A., Recanatini, M. & Valenti, P., Cholinesterase inhibitors: xanthostigmine derivatives blocking the acetylcholinesterase-induced beta-amyloid aggregation, *J. Med. Chem.* 48, 4444–4456 (2005).
46. Sterling, J., Herzig, Y., Goren, T., Finkelstein, N., Lerner, D., Goldenberg, W., Miskolczi, I., Molnar, S., Rantal, F., Tamas, T., Toth, G., Zagyva, A., Zekany, A., Finberg, J., Lavian, G., Gross, A., Friedman, R., Razin, M., Huang, W., Krais, B., Chorev, M., Youdim, M. B. & Weinstock, M., Novel dual inhibitors of AChE and MAO derived from hydroxy aminoindan and phenethylamine as potential treatment for Alzheimer's disease, *J. Med. Chem.* 45, 5260–5279 (2002).
47. Bolognesi, M. L., Cavalli, A., Valgimigli, L., Bartolini, M., Rosini, M., Andrisano, V., Recanatini, M. & Melchiorre, C., Multi-target-directed drug design strategy: from a dual binding site acetylcholinesterase inhibitor to a trifunctional compound against Alzheimer's disease, *J. Med. Chem.* 50, 6446–6449 (2007).
48. Bergmann, F., Wilson, I. B. & Nachmansohn, D., The inhibitory effect of stilbamidine, curare and related compounds and its relationship to the active groups of acetylcholine esterase. Action of stilbamidine upon nerve impulse conduction, *Biochim. Biophys. Acta* 6, 217–224 (1950).
49. Sugimoto, H., Ogura, H., Arai, Y., Limura, Y. & Yamanishi, Y., Research and development of donepezil hydrochloride, a new type of acetylcholinesterase inhibitor, *Jpn. J. Pharmacol.* 89, 7–20 (2002).
50. Kryger, G., Silman, I. & Sussman, J. L., Structure of acetylcholinesterase complexed with E2020 (Aricept®): implications for the design of new anti-Alzheimer drugs, *Structure* 7, 297–307 (1999).
51. Koellner, G., Kryger, G., Millard, C. B., Silman, I., Sussman, J. L. & Steiner, T., Active-site gorge and buried water molecules in crystal structures of acetylcholinesterase from *Torpedo californica*, *J. Mol. Biol.* 296, 713–735 (2000).
52. Josse, D., Ebel, C., Stroebel, D., Fontaine, A., Borges, F., Echalier, A., Baud, D., Renault, F., Le Maire, M., Chabrieres, E. & Masson, P., Oligomeric states of the detergent-solubilized human serum paraoxonase (PON1), *J. Biol. Chem.* 277, 33386–33397 (2002).
53. Aharoni, A., Gaidukov, L., Yagur, S., Toker, L., Silman, I. & Tawfik, D. S., Directed evolution of mammalian paraoxonases PON1 and PON3 for bacterial expression and catalytic specialization, *Proc. Natl. Acad. Sci. USA* 101, 482–487 (2004).
54. Rosenblat, M., Gaidukov, L., Khersonsky, O., Vaya, J., Oren, R., Tawfik, D. S. & Aviram, M., The catalytic histidine dyad of high density lipoprotein-associated serum paraoxonase-1 (PON1) is essential for PON1-mediated inhibition of low density lipoprotein oxidation and stimulation of macrophage cholesterol efflux, *J. Biol. Chem.* 281, 7657–7665 (2006).

55. Khersonsky, O. & Tawfik, D. S., The histidine 115-134 DYAD mediates the lactonase activity of mammalian serum paraoxonases, *J. Biol. Chem.* 281, 7649–7657 (2006).
56. Kuo, C. L. & La Du, B. N., Comparison of purified human and rabbit serum paraoxonases, *Drug Metab. Dispos.* 23, 935–944 (1995).
57. Roodveldt, C., Aharoni, A. & Tawfik, D. S., Directed evolution of proteins for heterologous expression and stability, *Curr. Opin. Struct. Biol.* 15, 50–56 (2005).
58. Sekar, K., Yu, B. Z., Rogers, J., Lutton, J., Liu, X., Chen, X., Tsai, M. D., Jain, M. K. & Sundaralingam, M., Phospholipase A2 engineering. Structural and functional roles of the highly conserved active site residue aspartate-99, *Biochemistry* 36, 3104–3114 (1997).
59. Scharff, E. I., Koepke, J., Fritzsch, G., Lucke, C. & Ruterjans, H., Crystal structure of diisopropylfluorophosphatase from *Loligo vulgaris*, *Structure (Camb)* 9, 493–502 (2001).
60. Waldo, G. S., Genetic screens and directed evolution for protein solubility, *Curr. Opin. Chem. Biol.* 7, 33–38 (2003).
61. Roodveldt, C. & Tawfik, D. S., Directed evolution of phosphotriesterase from *Pseudomonas diminuta* for heterologous expression in *Escherichia coli* results in stabilization of the metal-free state, *PEDS* 18, 51–58 (2005).
62 Radic, Z., Duran, R., Vellom, D. C., Li, Y., Chervenansky, C., & Taylor, P., Site of Fasciculin Interactions with acetylcholinesterase, *J. Biol. Chem.* 269, 11233–11239 (1994).